

REPORT DOCUMENTATION PAGE

Public reporting burden for this collection of information is estimated to average 1 hour per response, including the time for reviewing the data needed, and completing and reviewing this collection of information. Send comments regarding this burden including suggestions for reducing this burden to Department of Defense, Washington Headquarters Services, Directorate for Information Operations and Reports, Suite 1204, Arlington, VA 22202-4302. Respondents should be aware that notwithstanding any other provision of law, no person shall be held liable for any collection of information if it does not display a currently valid OMB control number. **PLEASE DO NOT RETURN YOUR FORM**

AFRL-SR-BL-TR-00-

0465

vis
with

1. REPORT DATE (DD-MM-YYYY) 31-07-2000		2. REPORT TYPE Final Report		3. DATES COVERED 1 Mar. 1997-31 Dec. 1999	
4. TITLE AND SUBTITLE On Braidability and Formability for 3D Braided Structural Shapes				5a. CONTRACT NUMBER NA	
				5b. GRANT NUMBER F49620-97-1-0160	
				5c. PROGRAM ELEMENT NUMBER	
6. AUTHOR(S) Albert S. D. Wang				5d. PROJECT NUMBER	
				5e. TASK NUMBER	
				5f. WORK UNIT NUMBER	
7. PERFORMING ORGANIZATION NAME(S) AND ADDRESS(ES) Drexel University 32 nd & Chestnut Streets Philadelphia PA 19104				8. PERFORMING ORGANIZATION REPORT NUMBER NA	
				10. SPONSOR/MONITOR'S ACRONYM(S)	
9. SPONSORING / MONITORING AGENCY NAME(S) AND ADDRESS(ES) AFOSR/NA 801 N. Randolph St. Arlington VA 22203				11. SPONSOR/MONITOR'S REPORT NUMBER(S)	
				12. DISTRIBUTION / AVAILABILITY STATEMENT Approval for Public Release; distribution unlimited.	
13. SUPPLEMENTARY NOTES					
14. ABSTRACT This final report outlines the research results obtained under the AFOSR Grant F49620-97-1-0160 for the period from 1 March 1977 to 31 December 1999. The research was partially augmented by the AASET Grant F49620-96-1-0283 for the period from 1 July 1997 to 31 December 1999. The main objective of the research was to develop a rational design/analysis methodology for a class of 3D braided structural shapes for aerospace applications. Research was carried out with two concurrent programs - the experimental program and the simulation program - involving design, braiding of preforms, consolidation and shape forming, fiber architecture determination and description, mechanics modeling, testing, investigation of preform braidability and formability at the consolidation stage.					
15. SUBJECT TERMS					
16. SECURITY CLASSIFICATION OF:			17. LIMITATION OF ABSTRACT	18. NUMBER OF PAGES	19a. NAME OF RESPONSIBLE PERSON Dr. Albert S. D. Wang
a. REPORT	b. ABSTRACT	c. THIS PAGE			19b. TELEPHONE NUMBER (include area code) 215-895-2297

ON BRAIDABILITY AND FORMABILITY FOR
3D BRAIDED STRUCTURAL SHAPES

Final Technical Report for Grants
F49620-97-1-0160 and F49620-96-1-0283 (AASERT)

Submitted to

Air Force Office of Scientific Research
Arlington, VA 22203

By

Albert S. D. Wang, PI
Department of Mechanical Engineering
Drexel University, Philadelphia PA 19104

- July 2000 -

This final report outlines the research results obtained under the AFOSR Grant F-49620-97-1-0160, which is in effect during the period from 1 March 1997 to 31 December 1999. The present research is also partially supported by the AASERT Grant F49620-96-1-0283 for the period from 1 July 1997 to 31 December 1999. Dr. Ozden O. Ochoa of AFOSR/NA is the Program Manager.

20000929 045

RESEARCH OBJECTIVE AND SCOPE

Background. The present research is aimed to further the technology concerning the design and analysis of three-dimensionally (3D) braided composites intended for aerospace structural applications. The research is stimulated, apparently, by the fact that 3D braiding with continuous yarns can produce preforms for structural members in their prescribed near-net-shapes; or if they are not, the preforms can be deformed into the prescribed near-net-shapes during consolidation with the matrix material; the final hardened composite members almost need no further machining; and, being endowed with 3D fiber reinforcement, the final products can possess a set of superior material toughness and damage-tolerant properties.

Engineering issues. However, there remain a host of technical challenges. From a rather limited perspective, these challenges can be loosely separated into two parallel classes. On one hand, there are issues concerning fabrication: (a) preform design – including yarn selection, preform shape, size and its internal fiber architecture, the associated braiding procedures, effective and possibly automated braiding apparatus; this then requires a rational methodology in order to insure the **braidability** of the intended preforms; (b) preform consolidation – including matrix material selection, the consolidation process and molding preparation in order to insure the optimal composite quality and the **deformability** of the preform which is to be consolidated to its prescribed shape.

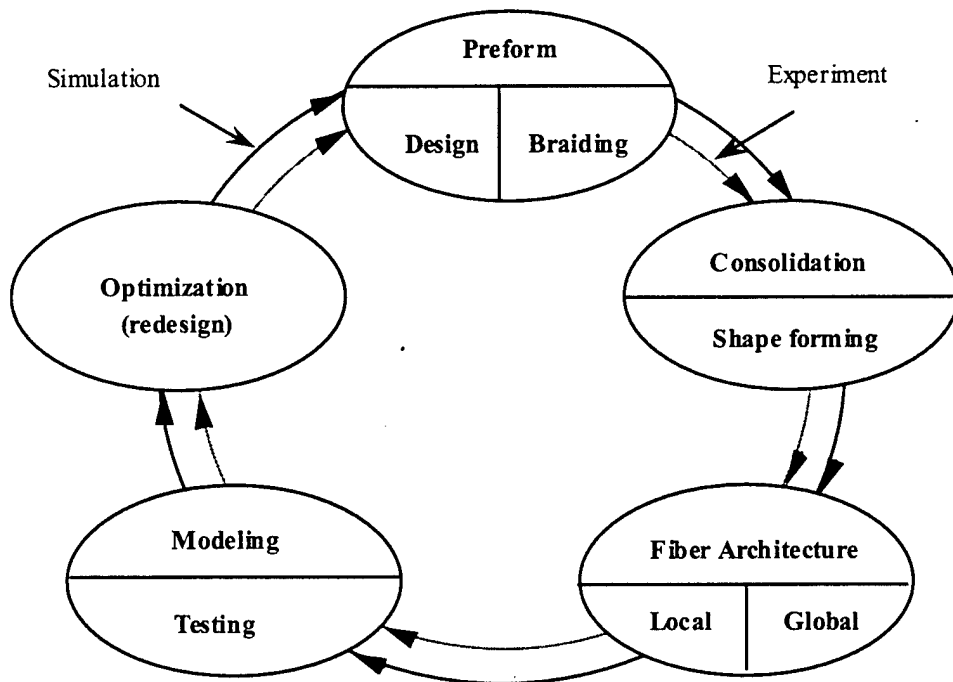
On the other hand, there are issues concerning analytical description and/or computer simulation of the various fabrication stages. Among these issues are: (a) braiding simulation – including most if not all of the influential material, geometry and kinematical parameters involved in the braiding process; the simulation must be able to mimic the entire process in a virtual-reality environment; such a process would insure the **braidability** of the designed preform, at least analytically; (b) analytical description of the 3D fiber reinforcement (architecture) in the braided (simulated) preform - including the characterization of the fiber architecture both locally and globally given the shape and braiding details of the preform; thus, the description must include most if not all of the material, geometrical and kinematical parameters involved in the braiding process; (c) analytical description of the fiber architecture when the preform is deformed during matrix consolidation – including both the local changes and the global shape deformation, given the details of the consolidation process; this would provide at least an analytical answer to the preform **deformability** question; (d) characterization of the composite properties - including the local properties as a material and the functional characteristics as a structural member under load.

These four elements of simulation form a closed-loop linking the various important stages of perform design and analysis. The latter can be used as a basis for developing an optimal design method for 3D braided composites.

Research Objective and Scope. The main objective of the research is to develop the aforementioned design/analysis loop in an analytical or virtual-reality environment for 3D braided composites; major elements in this loop include perform design, simulation of braiding, fiber architecture description, mechanics and structural modeling and optimization, with the particular emphasis on issues of preform braidability and deformability.

But, in order to correlate the developed simulation models, concurrent experiments are also performed; though the scope of the experimental work is limited, it is somewhat parallels to the analytical one; major elements in the laboratory work include the design and construction of braiding platforms, braiding of variously shaped specimens, their fabrication and consolidation, inspection of fiber architecture, testing of specimens to measure their local and global properties, and redesign and braiding of specimens of complex shapes.

Major elements in the parallel analytical/experimental loops are schematically shown in the figure below:



RESEARCH ACCOMPLISHMENTS

In this section, an outline of the experimental program and accomplishments is presented first; another for the analysis/simulation program follows. These outlines will briefly describe the nature of each of the key research and/or development topics in the programs, and the relevant results obtained therein; while the details in the conduct of these two parallel and correlative research programs are omitted in the outlines, frequent references are made of two publications which are appended to this report; namely, a Ph. D. dissertation, Ref. [1], and an overview article, Ref. [2]. Ref. [1] contains most of the details rendered in both of the programs of this research, while Ref. [2] provides a cohesive description of the variously developed links in the virtual simulation routine; it also lists 16 published papers by this research team.

The Experimental Program.

- **Construction of Braiding Platform.** The braiding apparatus for the present research was built at Drexel's Fibrous Materials research Laboratory; it is built based on the Magnaweave concept, with the 4-step procedure capable of braiding preforms with square or rectangular cross-sections. Two significant extensions of the original 4-step procedure were made: (a) a 8-step modified procedure which is capable of braiding preforms having cross-sections of L, T, I, U, and other complex shapes; however, the fiber architecture by the modified 8-step procedure is the same as that by the 4-step procedure (b) a modification of the braiding apparatus in order to add axial yarns in the braided preforms, using either the 4-step or 8-step procedures. Details of the platform construction as well as the modifications are found in Chapter II of Ref. [1].
- **Design and Braiding of Preforms.** The initial design of a preform requires several input parameters: the yarn selected, the braiding procedure, the exact preform geometry, etc. These input parameters allow the design for the yarn carrier deployment on the braiding platform (see section 2.3, Ref [1]). The question of preform braidability may come into play as well at this design stage, as an input from design simulation. Two classes of preforms were braided: (a) those of simple cross-sectional shapes, including square and rectangular sections braided by the 4-step procedure; both E-glass and graphite yarns (AS4-G2) were used in these braids; and (b) those having cross-sectional shapes of a hollow square, angle (L), channel (U), I-section and one resembling a 8-fin turbine blade were braided by the modified 8-step procedure; these braided specimens

contain various amount of axial yarns; only the graphite yarns were used in braiding this class of specimens. Details of the preform design, specimens braided and their dimensions are found in Chapter IV, Ref. [1].

- **Matrix Consolidation.** All braided preform specimens were consolidated with an aerospace grade epoxy resin (PR500) using the resin-transfer-molding (RTM) process. The RTM work was conducted jointly by Drexel University and Boeing Helicopters Co. Design and machining of the molds used in the process, the set-up and running of the RTM facilities were conducted by Drexel graduate students under the guidance of Boeing's facility engineers; in all more than 36 braided specimens were successfully consolidated. Details of the consolidation process are fully documented in chapter IV of Ref. [1].
- **Yarn Architecture Inspection.** In accordance with simulated yarn architecture study, the yarn structure (fiber architecture) in the braided specimen is totally characterized by three geometric parameters, which are inferred from three independent measurements of the specimen's surfaces. Thus, several consolidated samples were sectioned at different orientations in order to reveal their internal yarn structure and geometries. Visual examination of the sectioned specimens helped to provide a direct verification of the fiber architectures obtained in the simulated loop. In particular, visual examination verified the yarn structures in specimens with added axial yarns. Details of this part of the experiment as well as comparisons with the simulated results are documented in chapter III, Ref. [1].
- **Fiber Volume and Void Contents.** Samples of the consolidated specimens were taken for inspection of their fiber-volume-content and void-content. The fiber-volume-content was determined using the "acid digestion process" as described in the ASTM D-3171 standard; the void-content was determined by the so-called "pan method". The exact procedures in both of the inspections are documented in chapter IV, Ref. [1], along with the inspection results. The fiber-volume fractions determined from the samples were compared with that estimated based the simulated fiber architecture; and they were in good agreement as reported in chapter V, Ref. [1].
- **Mechanical Testing – Elastic Responses.** The consolidated specimens were tested for their mechanical and structural properties; among the properties sought were (a) the effective thermal elastic expansion coefficients; (b) the effective linear elastic constants;

and (c) the global flexural response under pure bending (i.e. 4-point bending). Special loading apparatus as well as data acquisition instruments were designed and setup for the tests; local strain measurements and global displacements were monitored and recorded in real-time. The test results were used to correlate with the simulated mechanics/structural models that were developed in the simulation loop. Details of the experiment and test data are found in chapter IV, Ref. [1]; while the correlative results with the variously developed predictive models have been presented in several technical papers, listed in Ref. [2].

- **Mechanical Testing - Failure Mode Study.** Selected 4-point bending tests were conducted till material damages occurred in the specimens; the failed specimens were then sectioned along some prescribed orientations and were examined visually under the scanning electronic microscope (SEM) for damage modes at the inter-yarn as well as the intra-yarn levels (i.e. damage modes in the fiber architecture). Study of failure modes helped to understand the physical mechanisms of load-transfer at the yarn level and the sub-yarn level; such understanding helps in turn to establish a rational failure model for the braided specimens loaded such as under pure bending. Description of the experiment is presented in chapter IV, Ref. [1], along with pertinent test results; correlative failure models are presented in chapter V, Ref. [1].

The Analysis/Simulation Program.

- **The Virtual Braiding Simulation.** Once a preform is designed, i.e. the preform cross-sectional shape, it's desired braided dimensions, the selection of the braiding yarn, the braiding procedures and the deployment of the braiding carriers are all finalized in the design, a geometrical method developed based on a control-volume concept is available which mimics the braiding motion of the yarns and provides a unique description of the spatial topology formed by the (virtually) braided yarns. This spatial yarn topology is geometrically characterized by three free-parameters whose values are to be determined after the preform is matrix-consolidated. In reality, the yarn topology is the precursor of the fiber architecture in the consolidated preform. It is noted that several braiding models were constructed during the research in order to validate the simulation routine. Much of the details of the routine have been presented in several technical papers published earlier, listed as 1, 7, 14 and 16 in Ref. [2] of this report. The virtual routine was applied manually to simulate all the 36 specimens braided in the experimental program. At the present time, the routine is being digitalized into a 3D "virtual reality"

computer program based on a concept similar to the finite element concept.

- **Identification of Unit-Cells.** Based on the virtually established yarn topology, repeated unit-cells in the braided preform, including cells in the interior and on the surfaces of the preform, can be identified by following the so-called “convected” coordinates that coincide with the braiding yarn lines. This novel approach identifies the smallest possible representative cells and their packing arrangement throughout the preform. For instance, the identified interior cell is only 1/8 the size of the cell identified by earlier researchers (see Ref. [2]). Furthermore, since the orientation of the cell coincides with the braiding yarn lines, the yarn topology of the cell can be totally characterized by the same free-parameters that characterize the topology of the entire preform. This is significant in two ways: (a) that smallest cell is also the simplest possible cell; it makes easier for a mechanics representation; and (b) that the smallest cell yields the most accurate properties when it is homogenized for determination of its stress/strain relation, or its effective material constitutive relation. On the other hand, the **packing** arrangement of the cells is analogous to a structure made of small building bricks; this then affords structural modeling of the preform when it is subjected to loading and/or global deformation.
- **Post-Consolidation Fiber Architecture – No Shape Change.** If the shape of the as-braided preform is unchanged during matrix-consolidation, e.g. a Cartesian cross-section remains a Cartesian, or a tubular cross-section remains tubular, then the three free-parameters that characterize the preform topology will assume fixed (constant) values after consolidation; the values are determined by three physical measurements (one length and two angles) all taken on the exterior surfaces of the consolidated piece; consequently, the entire fiber architecture of and the variously identified unit-cells in the consolidated piece can be precisely described. This part of the study was correlated with the experiment where several consolidated specimens were sectioned to reveal their actual yarn structures. The experimental validation of the simulated (virtual) fiber architecture along with its characterizing parameters is important in that the unit-cells in the consolidated piece are all defined, including their geometries and dimensions.
- **Post-Consolidation Fiber Architecture – With Shape Change.** If the shape of the as-braided preform is changed during matrix-consolidation, the fiber architecture in the consolidated piece will change from that in the as-braided preform. To account for such changes, a geometric mapping method was developed which maps the yarn topology in

the as-braided preform to the fiber architecture in the consolidated and deformed piece. Based on this method, the mapping can be uniquely determined only if the deformation is “physically permissible”; the latter translates to a set of geometric conditions to be imposed upon the mapping function. The result of the mapping is that the fiber architecture in the deformed piece is completely characterized by the same three parameters that characterize the yarn topology of the as-braided preform; but the values of the parameters may vary from location to location inside the consolidated piece, depending on the nature of the imposed deformation. Significantly, the three spatially varying can be uniquely determined from measurements taken the exterior surfaces of the consolidated piece. Again, determination of the spatially-dependent parameters is important in that the unit-cells in the consolidated piece are all defined, including their geometries and dimensions; the latter may also vary as function of location. This part of the study has been reported in several technical papers, listed as 1, 2, 5 and 6 in Ref. [2].

- **Modeling Mechanical Properties – Local Cells.** The general approach adopted here is to represent the local unit-cell as a material-volume endowed with a set of “effective” elastic constants. Here, the unit-cell is replaced by a “homogenized volume element”, a concept similar to that used in treating conventional unidirectionally fiber-reinforced composites. Since the local unit-cell and the yarn geometries in the cell are all known, an appropriate micromechanics model may be used to extract the effective (elastic) constants for the unit-cell (see chapter V, Ref. [1]; or papers listed as 3, 4, 7, 8, 9, 11, 13 and 15 in Ref. [2]). It is noted that the various unit-cells vary in their shape, dimensions and yarn structures; the modeled composite piece (i.e. the consolidated preform) is not a homogeneous material.
- **Modeling Mechanical Properties – Global Response.** By global response, it refers to structural response of a load-bearing member (e.g. the consolidated preform under load) to specifically applied load, which may be both mechanical and/or thermal. Here, a structural model is constructed for the entire consolidated preform based on its unit-cell composition, where both the individual cells and the cell packing order are previously determined from the simulated fiber architecture. And, each cell is already represented by a volume element with a set of effective elastic constants. Thus, the cell composition resembles a 3D finite-element model for the entire member; and it can be executed on numerically on the computer and the global responses of the specimen determined under the specifically applied. All of the consolidated specimens tested in the

experiment were independently analyzed by this approach; comparison between the simulated responses and the responses recorded experimentally were more or less agreeable. Most of the detailed are contained in Chapter 5, Ref. [1] and papers listed as 8 and 15 in Ref. [2].

- **Mechanisms-Based Failure Criterion.** In the experimental investigation, several consolidated specimens were tested to apparent failure initiation under 4-point bending; the damaged specimens were then sectioned and examined under SEM to delineate the dominant damage modes and the mechanisms in which damage occur. Simultaneously, with the developed structural model, the global response of the loaded specimen is linked to the various local cells; and with the micromechanics, calculation can be made for the stress state of the cell, including yarn tension, compression and inter yarn stress-transfer. Thus, the initial failure under pure bending could be described and simulated based on the identified damage mode and mechanism; namely, the inter-yarn shearing within the unit-cells located inside the compressive zone of the specimen. The formulation details are presented in papers listed as 13 and 15 in Ref. [2], and more fully with supporting SEM results in chapter V in Ref. [1].
- **Preform Braidability and Deformability.** With the above developed design/analysis loop, and in particular the geometric yarn mapping method, the subjects of preform braidability and deformability were studied in a virtual reality environment. Here, braidability refers to the possibility that a preform of a certain prescribed shape is actually braidable without violating the external shape limitation and the internal braiding yarn constraints; while deformability refers to the permissible deformation that a preform can sustain without incurring internal damage or violating inter-yarn constraints, including yarn stretching, buckling and/or inter-yarn shearing. In this research, the subject of preform deformability was studied more extensively, however. Some specific results were presented in several papers listed as 6 and 10, Ref. [2].

References Cited in and Attached to This Report:

[1] Kumar, Amrita. 1999. "*On design, yarn architecture and mechanical behavior of 3D braided composites*", Ph. D. Dissertation, Drexel University.

[2] Wang, A. S. D. 2000. "*A Design and Analysis Methodology for 3D Braided Structural Shapes*", Proceedings, American Society for Composites 15th Annual Meeting.

APPENDICES

[1] Amrita Kumar "*On Design, Yarn Structure and Mechanical Behavior of 3D Braided Composites*," Ph. D. Dissertation, Drexel University. 1999*.

* This document has been submitted to AFOSR/NA separately.

[2] A. S. D. Wang "*A design and Analysis Methodology for 3D Braided Structural shapes*," *Proceedings of American Society for Composites, 15th Technical Meeting, September, 2000.*

A DESIGN AND ANALYSIS METHODOLOGY FOR 3D BRAIDED STRUCTURAL SHAPES

A. S. D. Wang
Drexel University
Philadelphia, PA 19104

ABSTRACT

This paper presents the highlights in a design-and-analysis methodology developed for three-dimensionally (3D) braided composites of bar-like bodies, having complex cross-sectional shapes. The highlights include (a) virtual design and virtual braiding of preforms with the prescribed cross-sectional shapes by the 4-step 1x1 procedure; (b) geometric description of the 3D fiber architecture in the virtually braided preforms; (c) description of the fiber architecture after preform matrix consolidation, a process in which the preform's initial cross-sectional shape may be altered; and (d) mechanics modeling approaches for the local and global properties of the matrix-consolidated composite members. These analytical developments are intrinsically connective; and they provide the basis for a closed-loop design-analysis methodology.

INTRODUCTION

A class of textile composites, fabricated by three-dimensional (3D) braiding, has been studied by the present author and his coworkers [1-16]. Briefly, several groups of fibrous preforms were designed and braided by the 4-step 1x1 method using high-modulus glass and graphite yarn systems; the general configuration of the preforms was that of a bar-like member with uniform but complex cross-sectional shapes; the preforms were consolidated with an epoxy resin by the transfer molding process; the cross-sectional shapes of most of the preforms were kept unchanged but a few were deformed intentionally during consolidation; the consolidated members were tested under various loading conditions, with local and global load-deformation properties measured and compared with their counter-part results predicted by analytical models.

In this paper we present the highlights of our earlier works, relating only to aspects of preform design, braiding, description fiber architecture in preforms before and after matrix consolidation, and modeling approaches for local and global properties of the consolidated composite members. In particular, our discussion will be conducted in a virtual environment; no experimental result will be presented. Much of the latter can be found in our previous publications [8, 13-15].

DESIGN, BRAIDING AND FIBER ARCHITECTURE.

The standard "4-step 1x1" braiding procedure was due to a patent filed by Florentine [17]. The procedure can braid bar-like preforms on a set of Cartesian tracks with uniform solid cross-sections, including squares or rectangles; preforms of uniform tubular cross-sections can also be braided on a set of hoop-and-radial tracks. Kumar [14] modified the 4-step procedure to 8-steps and braided preforms on a Cartesian track with cross-sections having inner corners, such as angles (L), tees (T), channels (U), hollow squares and wide-flange sections (H). Preforms braided by the modified 8-step procedure possess identical fiber architecture topology as that produced by the standard 4-step procedure.

Axial yarns can be added in the preform in order to strengthen the axial stiffness [14]. The axial yarns do not braid themselves and do not interfere with the moves of the braiding yarns; they add complexity in the fiber architecture, however [9,14].

Shape Design and Braiding Parameters.

The preform cross-sectional shape is related directly to the pattern of yarn carriers deployed on the braiding tracks. The cross-sectional dimensions, however, depend on a number of other factors: yarn size, numbers of yarn carriers deployed in the shape pattern, the degree of yarn jamming during the braiding cycles, etc. In what follows, we use a preform with the rectangular cross-section as an example in order to illustrate the interrelationships that connect shape design, dimensions of the as-braided preform, and the geometric yarn architecture visualized on the surfaces of the as-braided preform and inferred in it's interior.

A rectangular cross-section is braided on a set of Cartesian tracks; the nominal size of the braided preform is designated as $M \times N$; namely, there are M horizontal (x) tracks and N vertical (y) tracks. Here, $[(M \times N) + (M + N)]$ carriers need to be deployed on the tracks; $M \times N$ carriers fill the domain of the intended rectangle; $(M + N)$ carriers are deployed outside the domain; see e.g. [1] for details. After each 4-step braiding cycle, a finite length of the preform is braided, known as a pitch. Fig.1a shows the exterior look of a rectangle preform after several braiding cycles.

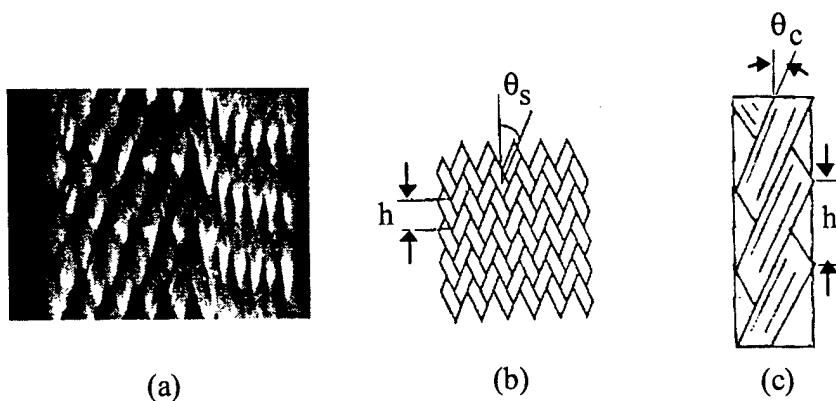


Fig.1 (a) Exterior look of the braided piece; (b) yarn topology at surface and corner; (c) yarn topology at corner.

Note the yarn geometric pattern on the surfaces of the preform. Major characteristics are illustrated in Fig.1b and 1c: Note the yarn size, angle formed by the crisscrossing yarns and the braiding pitch h , as shown in Fig.1b; not the unique yarn pattern at the preform corner, Fig.1c. These physical factors can be measured from the as-braided preform. For instance, the sides of the rectangle W_x and W_y , and the braiding pitch h can be easily measured; then, the crisscrossing yarn angle θ_x on x-face and θ_y on y-face are determined:

$$\theta_x = \tan^{-1}(\Delta x/h); \quad \Delta x = W_x/N \quad (1)$$

$$\theta_y = \tan^{-1}(\Delta y/h); \quad \Delta y = W_y/M \quad (2)$$

Similarly, the yarn angle at the corners, Fig.1c, can also be determined as:

$$\theta_c = \tan^{-1}(2d/3h); \quad d = \sqrt{(\Delta x^2 + \Delta y^2)}/2 \quad (3)$$

where d is the center-to-center spacing between two adjacent yarns.

Since most preforms are braided under uniform yarn jamming, then $\Delta x = \Delta y$, $\theta_x = \theta_y$ and $d = \Delta x / \sqrt{2}$. When consolidated with matrix, the preform may be stretched axially and pressed more on one side than the other; then, new measures must be made of W_x , W_y and h . In that case, Δx and Δy may differ; but the relations (1-3) remain valid.

In preform design, the braiding yarn is selected priori. Experience with the selected yarn would then provide a narrow value-range for yarn spacing d . In the example of the rectangle, the required values of M and N can then be estimated using the relations in (1-2), if the consolidated preform size W_x and W_y is desired. Similarly, given the braiding yarn, a value-range for the braiding pitch h can also be defined empirically; this then allows control of the surface angles θ_x , θ_y and θ_c through the control of h .

The above design guidelines can be applied to cross-sectional shapes other than a rectangle, so long as the preform is braided on a set of Cartesian tracks.

When axial yarns are added to the basic braiding defined by $M \times N$, the values of W_x , W_y and h will increase with the amount of the axial yarns added; the relations in (1-2), however, still will remain valid [14].

Fiber Architecture in the Interior.

The fiber architecture in the preform interior is not easily visualized, especially when the preform is matrix-consolidated. Traditionally, the interior fiber architecture has been identified by destructive methods involving specimen dissection, see e.g. Li [18]. Wang, et. al. [1,4] developed a "virtual control space"

technique which traces the yarn paths in and out of the control space during a virtual braiding cycle; the yarns that remain inside the control space then furnish the exact architecture topology for both the interior and the surfaces of the preform.

Since the basic yarn architecture topology is unique to the braiding method used, all preforms braided by the 4-step or the 8-step procedure possess the same basic fiber structure. As the preform interior nestles continuously with its surfaces, the same surface measurements (W_x , W_y , h) will characterize geometrically the entire fiber architecture, including the interior. This is best explained at two descriptive levels: First, the interior is spanned by two groups of parallel plates, labeled $\pm\alpha$ -plate in Fig.2a; these plates crisscross at the angle 2α , α being measured from the x-axis to the α -plate. thus, in preforms braided under uniform yarn jamming, $\alpha=45^\circ$; so the two sets of plates intersect orthogonally. Secondly, the yarn structure in the α -plate is formed by two groups of parallel yarns crisscrossing at the angle 2γ (γ is measured from the y-axis to the axis of the yarn), Fig.2b.

If the center-to-center spacing of adjacent yarns is d , then the thickness of each plate is $2d$. Fig.2c shows a section cut from a matrix-consolidated preform along the mid-plane of an α -plate; it reveals how the $\pm\alpha$ -plates intersect as seen in the cut plane. From geometry [1], it can be shown that angles α and γ which characterize the interior yarn structure are related to the three surface measurements in the following manner:

$$\alpha = \tan^{-1}(\Delta x/\Delta y) \quad \gamma = \tan^{-1}(4d/h) \quad (4)$$

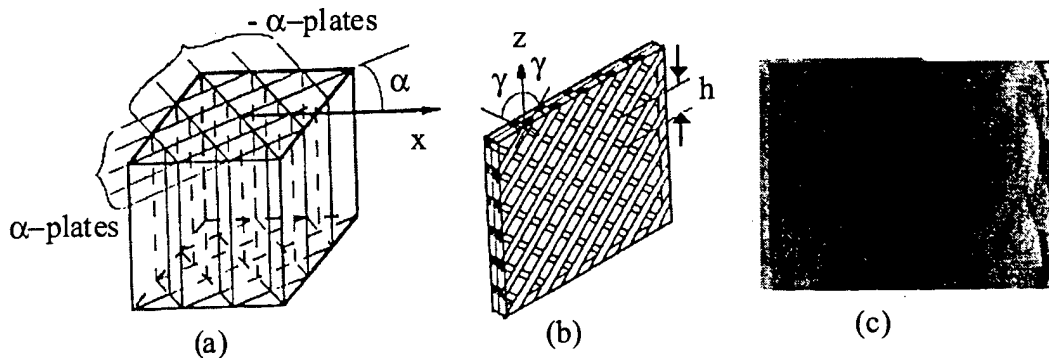


Fig. 2. (a) The interior fiber structure; (b) the structure of the α -plate; (c) a picture of the braided piece sectioned along the α -plane.

Of course, the fiber architecture in matrix-consolidated preform is described by the same three exterior measurements taken after consolidation, so long as the general shape of the preform cross-section is preserved during consolidation.

MAPPING OF FIBER ARCHITECTURE DUE TO PREFORM DEFORMATION.

If the as-braided cross-sectional shape is deformed during consolidation, the general topological nature of the yarn structure in the deformed preform does not change provided that the deformation is physically permissible. Depending on the specifics in the deformation, the characterizing parameters (α , γ and h) may change their values and they may differ from location to location. The point here is that the yarn architectures in the as-braided and the deformed configurations are connected by a unique mapping.

This issue, however, cannot be discussed in full without being specific. So, for definiteness, let us return to the example considered earlier, MXN rectangle (shown as B_0 in Fig.3a) where the fiber architecture is already characterized by α_0 , γ_0 and h_0 . Now, let the preform be stretched axially so the pitch h_0 becomes h ; and let the cross-section B_0 be deformed to the cross-section B , Fig.3b. If the preform thickness W_y is much smaller than the width W_x , then the thickness W_n in B is linear but can vary along t ; the width W_t may vary along both t and n . In general, the curvilinear coordinates (t,n) in B are not orthogonal and the local angle ϕ formed by t and n vary with t .

With the above, the objective is then to obtain the mapping that takes the point (x,y) in B_0 to the corresponding point (t,n) in B , together with the fiber architecture which is endowed in the respective bodies. Of course, the desired mapping must be one which is physically permissible and yields unique values of α , γ and h for the fiber architecture in B .

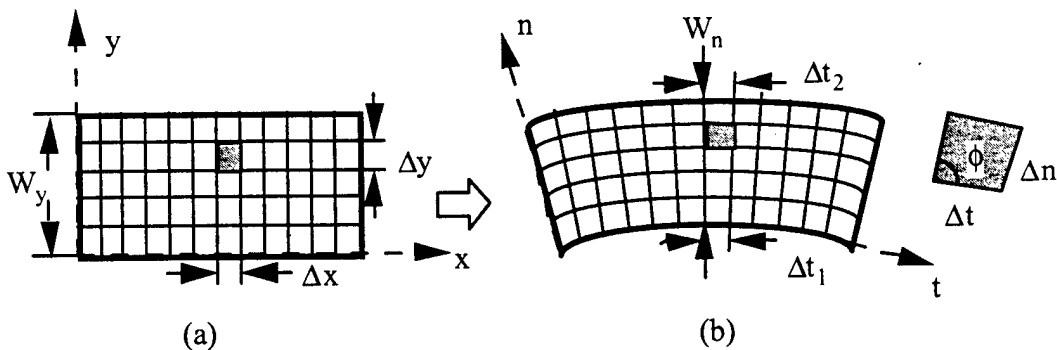


Fig.3. (a) the as-braided cross-section; (b) the deformed cross-section

Now, let the following be measured from the deformed preform B : the braiding pitch h , local $\Delta t_1(x)$ on the bottom surface $n=0$ and $\Delta t_2(x)$ on the top surface $n=W_n(x)$ which correspond to the length of Δx at x in B_0 , and the local thickness $W_n(x)$ in B which correspond to the location x in B_0 . Thus, the desired mapping is in the general form:

$$t = f(x,y) \quad n = g(x,y) \quad \zeta = h_0/h. \quad (5)$$

where the mapping functions $f(x,y)$ and $g(x,y)$ are determined by the following:

From the geometry of the local volume element $(\Delta x \Delta y)h_0$ in B_0 and $(\Delta t \Delta n)h$ in B , together with the constraint that the yarns in the elements are inextensible, a set of first order partial difference equations are obtained (see [2] for details):

$$\Delta x / \Delta t = 1 / (\lambda_1 + kn) \quad (6)$$

$$\Delta y / \Delta n = \{ (\lambda_1 + kn) \cot \alpha_0 \cos \phi + \sqrt{ [m^2 \csc^2 \alpha_0 - (\lambda_1 + kn)^2 \cot^2 \alpha_0 \sin^2 \phi] } \} / [m^2 \csc^2 \alpha_0 - (\lambda_1 + kn)^2 \cot^2 \alpha_0] \quad (7)$$

where

$$\lambda_1(x) = \Delta t_1(x) / \Delta x \quad k = [\lambda_1(x) - \lambda_2(x)] / W_n(x)$$

$$m^2 = (1 - (\zeta^{-2} - 1) \cot^2 \gamma_0) \quad (8)$$

We first integrate partially (7) over n , which yields the expression for $y(x, n, \phi)$; the boundary values of the thickness W_y in B_0 and $W_n(x)$ in B are then used to determine the expression for the local angle $\phi(x)$. This then reduces the expression for y to $y(x, n)$ only; the inversion of which gives $n=f(x,y)$. Next, we substitute $n=f(x,y)$ in (6) and integrate partially over t at the discrete points where $\lambda_1(x)$ and $\lambda_2(x)$ are measured; an expression for $t = g(x,y)$ is obtained.

With the mapping functions $n=f(x,y)$ and $t=g(x,y)$ determined, the fiber architecture in B is then characterized by the parameters α , γ and h :

$$h = h_0 / \zeta \quad \cos \gamma = \cos \gamma_0 / \zeta \quad \sin \alpha = (\sin \phi / m) (\Delta n / \Delta y) \sin \alpha_0 \quad (9)$$

In this case, h and γ are uniform in B ; but α varies with t . This means that the $\pm\alpha$ planes are curved in B . The yarn-to-yarn spacing d in B becomes:

$$d = [(\Delta t / \Delta x) (\Delta n / \Delta y) \sin \phi / m] d_0 \quad (10)$$

For the deformation B to be physically permissible, the value of d must be within the prescribed value-range for yarn spacing associated with the yarn used in the braiding. The latter is related to the issue of preform deformability, which has been discussed in more details in [6,10].

MECHANICS AND STRUCTURAL MODELING APPROACHES.

In the present context, mechanics modeling is to formulate a theoretical framework from which mechanical properties of a local material volume can be extracted based on the fiber/matrix materials endowed therein. If the properties of all such local material volumes are extracted throughout the consolidated member, then a

structural model is needed by which the responses of the member under the applied load can be predicted. Hence, the first order is to identify the material volume which is the smallest and yet representative of the braided preform.

Unit-Cells in Preforms by the 4-Step 1x1 Method.

Fiber architecture in preforms can always be represented as a composition of repeated unit-cells, since these cells are formed and repeated in each and every braiding cycle. For purpose of mechanic modeling, the yarn structure in each cell as well as the packing order of the cells in the preform cross-section must be identified correctly and consistent with the overall fiber architecture. For preforms braided by the 4-step 1x1 method, the repeated unit-cell is physically large and contains a fairly complex yarn structure. Fig.4a shows the unit-cell packing order in the preform cross-section; each unit-cell is orientated parallel to the $\pm\alpha$ -planes (this unit-cell was first identified by Li [18]); it has a dimension of $4d \times 4d \times h$ and contains 16 yarn segments.

Wang, et. al [1] represented the repeated unit-cell by 8 smaller sub-cells, 4 A-cells and 4 B-cells, which are packed in a checker-board fashion as shown in Fig.4b. The size of sub-cell A or B is $2d \times 2d \times (h/2)$; it contains just two crisscrossing yarns with the angle 2γ , Fig. 3c. It is noted that A-cell and B-cell are topological independent; i.e. one cannot represent the other.

Finally, let A_f be the solid cross-section area of the braiding yarn; the fiber volume content in the sub-cells is given by:

$$V_f = A_f / (\Delta x \Delta y \cos \gamma) \quad (11)$$

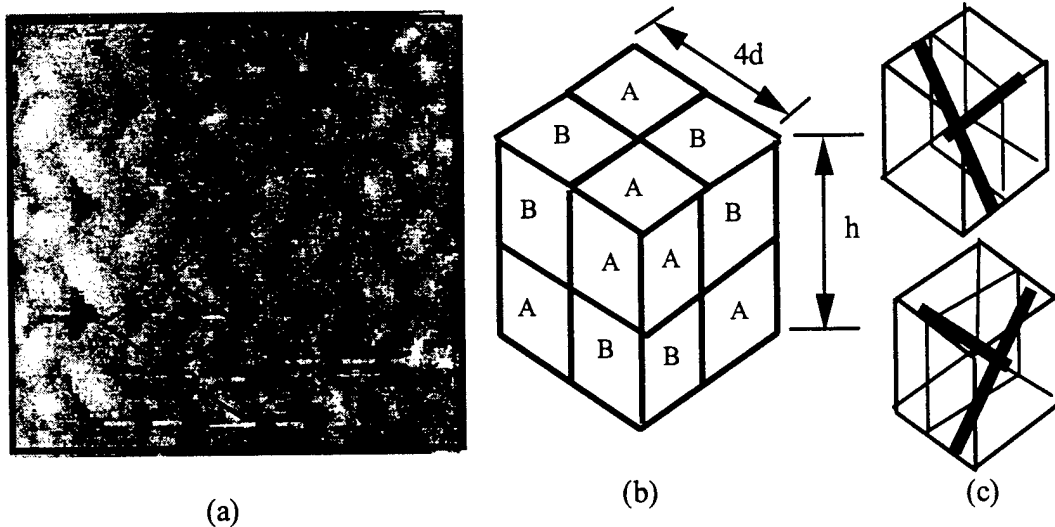


Fig. 4. (a) Yarn pattern in preform cross-section with identified unit-cell; (b) The unit-cell consisting 8 sub-cells; (c) Yarns in A-cell (top) and B-cell (bottom)

Modeling Approaches for Properties.

Note that sub-cell A is essentially a small element taken out of the α -plate, and B is taken from the $-\alpha$ -plate; both of the plates resemble a $[\pm\gamma]$ laminate. A or B is small in size and simple in the yarn structure; hence, the local properties may be extracted by some traditional methods of homogenization [3,12], based on a cross-ply laminated theory [19]; alternatively, A or B can be modeled by some micromechanics methods that distinguish the fiber and matrix as separate materials, e.g. [4,11].

In either case, the sub-cells can be treated as 3D finite elements, with the nodal forces and displacements related by the stiffness matrix endowed therein. A global analysis can then be carried out by the usual finite element method for the overall member under load. Detailed development in some earlier studies can be found elsewhere and will not be repeated here.

Acknowledgments: Results reported herein have been obtained through the research supported by AFOSR; the author acknowledges the contributions made by his coworkers: Drs. Youqi Wang, Soheil Mohajerjasbi and Amrita Kumar.

REFERENCES.

1. Wang, Y. Q. and A. S. D. Wang. 1994. "On the Topological Yarn Structure in 3-D Rectangular and Tubular Braided Preforms," *J. Composites Science & Technology*, 51: 575-586.
2. Wang, Y. Q. and A. S. D. Wang. 1994. "On Topological Mapping of Yarn Structures in 3-D Braided Composites," Proc. of the American Society for Composites, 9th Technical Conference, Technomic Publishing Co., pp. 869-876.
3. Wang, Y. Q. and A. S. D. Wang. 1995. "Microstructure-Property Relationships in 3-D Braided Composites," *J. Composites Science & Technology*. 53: 213-222.
4. Mohajerjasbi, S. 1994. "Structure and Mechanical Properties of 3-D Braided Composites," Ph.D. Thesis, Drexel University.
5. Wang, Y. Q. and A. S. D. Wang. 1995. "Geometrical Mapping of Yarn Structures Due to Shape Change in 3-D Braided Composites," *J. Composites Science & Technology*, 54: 359-370.
6. Wang, Y. Q. and A. S. D. Wang. 1995, "Yarn Structures in 3-D Braided Composites Due to Complex Shape Change," *Recent Advances in Composite Materials*, ASME MD-65, Ed. S White, T Hahn and W. Jones. pp. 151-161.
7. Wang, Y. Q. and A. S. D. Wang. 1995. "Spatial Distribution of Yarns and Thermo-mechanical Properties in 3-D Braided Tubular Composites," *Proc. ICCM-10, Canada*, 4: 285-292.
8. Wang, A. S. D. and S. Mohajerjasbi. 1995. "Thermoelastic Properties of 3-D Braided Composites: Predictions and Experiment," *Innovative Processing and Characterization of Composite Materials*, ASME AMD-211, Ed. R. Gibson, T. Chou and P. Raju. pp. 275-293.

9. Mohajerjasbi, S. 1995, "Structure and Properties of 3D Braided Composites including Axial Yarns," *AIAA Journal*, 34(1): 209-211.
10. Wang, Y. Q. and A. S. D. Wang. 1996. "Formability of 3-D Braided Composites." *Proc. ICAM-96 China*, Peking University Press. pp. 160-167.
11. Mohajerjasbi, S. 1997. "Predictions for Coefficients of Thermal Expansion of 3D Braided composites," *AIAA Journal*, 35(1): 141-144.
12. Wang, Y. Q. and A. S. D. Wang. 1997. "Spatial Distribution of Yarns and Mechanical Properties in 3-D Braided Tubular Composites," *Jour. Applied Composite Materials*, 4: 121-132.
13. Wang, A. S. D. and A. Kumar. 1997. "Stiffness and Strength Properties in 3-D Braided Structural Composite Shapes," *Proc. ICCM-11*, Australia. pp. 379-386.
14. Kumar, A. 1998. "On Design, Yarn Architecture and Mechanical Behavior of 3D Braided Composites," Ph.D. Thesis, Drexel University.
15. Wang, A. S. D. and A. Kumar. 1998. "Local and Global Properties in 3-D Braided Structural Shapes," *Proc. 8th Japan-US Conference on Composite Materials*. pp.157-166.
16. Mohajerjasbi, S. 1998. "Fiber Architecture of 3D Braided composites," *AIAA Journal*, 36(4): 613-617.
17. Florentine, R. 1982. "Apparatus for Weaving a Three-Dimensional Article," U. S. Patent No. 4,312,261.
18. Li, W. 1990. "On the Structural Mechanics of 3D Braided preforms for Composites," Ph. D. Thesis, North Carolina State University.
19. Pagano, N. J. 1974. "Exact Moduli of Anisotropic Laminates," *Mechanics of Composite Materials*, Edited by G. P. Sendeckyj, Academic Press, New York. p.23.